Proceedings of ERAD (2004): 335–340 © Copernicus GmbH 2004

ERAD 2004

# Experiments on using the Sun for radar calibration

**P. Puhakka, M. Leskinen, and T. Puhakka**

Division of Atmospheric Sciences, P.O. Box 64 (Gustaf Hällströminkatu 2), FIN-00014 University of Helsinki, Finland

**Abstract.** A brief theoretical background to the possibilities for using the Sun in weather radar calibrations is given. As an example, Sun measurements with the University of Helsinki C-band Doppler weather radar are compared to the results obtained using the laborious standard gain horn method. Results show that both Sun measurements and horn measurements give similar beam widths. The main advantages of the Sun measurement are, that it is fast and much easier to perform than the horn beam pattern measurement, results can be obtained from different elevation angles and the method can be used for both horizontal and vertical polarization. Moreover, though the method used in this study uses a stationary antenna, some indications of the ellipticity of the beam can be obtained. Variations in the activity of the Sun may cause problems in the interpretation, but fortunately, suspicious cases may be detected from the data in most cases.

## 1 Introduction

The calibration of a weather radar includes a determination of the characteristics of four main subsystems: transmitter, antenna, receiver/processor and the waveguide assembly. Each of these contains many different aspects to be considered. As a consequence, the complete calibration of a radar is a complex and laborious task, involving many kinds of laboratory test instruments and setups.

Two main technical developments during recent decades have considerably improved the possibility of achieving an accurate calibration: The adoption of digital techniques in the receivers/signal-processors, and improved electrical stability in the remaining analogue parts of the radar.

On the other hand, use of more complicated techniques, like polarimetry, requires more accuracy and even completely new aspects to be calibrated and monitored. The required accuracy cannot be easily achieved in a straightforward manner by measuring all parts of the signal routes from the transmitter to the antenna and from the antenna to the receiver/processor, and then summing the results. This is because the errors in the individual measurements add up. Another disadvantage of this kind of method is that it is difficult or even impossible to automatize for operational purposes. This has led to different kinds of bulk-calibration methods, such as using the Sun or echoes from precipitation to calibrate the signal routes as a whole.

*Correspondence to:* P. Puhakka
(pekka.puhakka@helsinki.fi)

The Sun cannot be used in transmitter calibration, but it is useful in the calibration of the antenna, the signal route from the antenna to the receiver and to some extent the receiver itself. The Sun has so far mainly been used for calibration of the pointing angles of the antenna (Whiton et al., 1976; Arnott et al., 2003). In principle it may also be used to determine the half-power beam width (HPBW) of the antenna (Kuz'min and Salomonovich, 1966; Leskinen et al., 2002; Frush, 1984) and even the antenna gain (Whiton et al., 1976). The Sun is also important in calibrating or balancing receiving chains from the antenna to the final output of the signal processor as a whole in a multi-channel receiver system (Hubbert et al., 2003; Frush, 1984). This paper concentrates on using the Sun to perform antenna beam calibration.

## 2 Measurements and analysis

### 2.1 Sun measurements

The University of Helsinki radar used in this experiment is a C-band Doppler weather radar (WSR81C-D manufactured by Enterprise Electronics), which has been operated since 1984 in the centre of Helsinki. According to the measurements made at the factory in 1983, the HPBWs of its parabolic 4.3 m dish without the radome were 0.89° and 0.97° in the horizontal and vertical direction respectively, and the antenna gain was 44.4 dB. First side lobes were 23 dB...20 dB below the main lobe maximum. According to

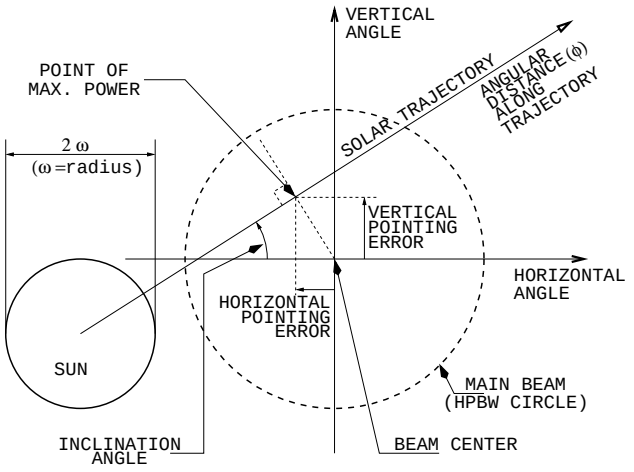


**Fig. 1.** Geometry of single solar passage. Vertical and horizontal angles are in antenna beam co-ordinate system.

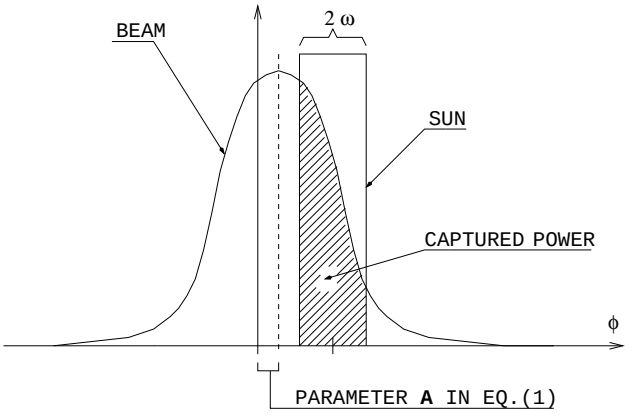


**Fig. 2.** Illustration of the power captured by Gaussian beam from a circular Sun.

the manufacturer's specification, the transmission loss of the 5.5 m radome was less than 0.5 dB.

The Sun measurements were done by holding the radar antenna stationary pointing somewhere close to the track of the Sun, and measuring the received power as a function of time while the Sun was passing. This means that only one inclined track was measured at a time.

The analogue logarithmic receiver was used in this experiment. The power received was estimated by integrating digitally an equivalent of 12 800 samples of the incoming signal. One estimate took roughly 0.15 s. During each solar passage, values of the received power were recorded at 15 s intervals, corresponding to an angular resolution of roughly 0.06°. On average a single passage took 8 minutes to complete; during this the Sun travelled an angular distance of 2° (one degree towards and one degree away from the radar pointing location).

The geometry of a solar passage is illustrated in Fig. 1. The azimuth and elevation co-ordinates of the Sun were extracted from SOLPOS (2004). These were trigonometrically converted into the angular position $\phi$ in the antenna beam co-ordinate system. Since there may have been some pointing error present, the track did not necessarily pass through the centre of the beam

Measurements were made on 53 occasions during the year 2002. The data set thus represents a variety of differently-inclined crossings at various elevation and azimuth angles.

The method of estimating the beam parameters was based on the assumption of a circular Gaussian antenna main lobe. Assuming the Sun to be a circular disk of known radiation pattern on a known background, the power captured by the Gaussian main lobe of the antenna can be theoretically calculated for any beam width and any location of the Sun as it passes the beam (Fig. 2).

Two slightly different methods were used to calculate the captured power. In both methods it was estimated theoretically by multiplying the intensity of the solar radiation at each point of the solar disk by the assumed normalized Gaussian beam pattern, and by integrating the result over the whole solar disk. In the first method derived by Puhakka (2002) and explained in more detail in Leskinen et al. (2002), the integration was performed analytically. The resulting solution for the power $P$ received by the antenna is

$$P = \int_{\phi-\omega}^{\phi+\omega} I(\phi) e^{-B(\phi-A)^2} d\phi = I \int_{\phi-\omega}^{\phi+\omega} e^{-B(\phi-A)^2} d\phi$$
$$= \frac{I}{2}\sqrt{\frac{\pi}{B}} \left( \mathrm{erf}\left(\sqrt{B}\,(\phi - A + \omega)\right)\right)$$
$$-\frac{I}{2}\sqrt{\frac{\pi}{B}} \left( \mathrm{erf}\left(\sqrt{B}\,(\phi - A - \omega)\right)\right), \quad (1)$$

where $I(\phi)$ is the radiation intensity of the Sun as a function of angle $\phi$ (the angular position of the Sun along the trajectory through the antenna beam). Since the radiation is assumed to be constant, it is replaced by $I$ and taken outside the integral. $B$ is the parameter defining the HPBW $= 2 \cdot \sqrt{\ln(2)/B}$, and $A$ is the offset of the peak from $\phi = 0$ (this offset is caused by the pointing errors illustrated in Fig. 1). $\omega$ is the angular radius of the Sun (1.07 times larger than the optical radius, according to Kuz'min and Salomonovich, 1966). The assumptions made to obtain Eq. (1) are: the Sun is circular and passes exactly via the centre of the beam, which is circular and Gaussian. The receiver is assumed to perform ideally logarithmically (or linearly) without any noise.

In the other solution by Leskinen et al. (2002), numerical integration was applied. In the numerical solution the intensity distribution over the Sun $I(\phi)$ is not necessarily constant but can be varied.

In both methods the antenna beam widths were now varied until the beam width was found for which the differences between the theoretically-estimated powers and the corresponding measured values were minimized.

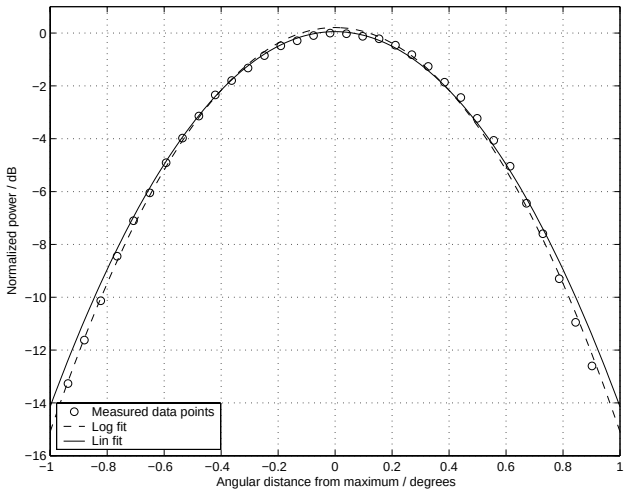


**Fig. 3.** A typical example of theoretical power distributions having the minimum difference compared to the measured power distribution (open circles) during a solar passage. Continuous line is the result using linear and dashed line using logarithmic minimization.

Differences were minimized both on a linear scale and on a logarithmic scale. According to the results, linear minimizing gave systematically larger beam widths than logarithmic. The reason for the difference is demonstrated in Fig. 3. In linear minimization, the differences in the highest power values (i.e. those obtained when the Sun was at or close to the centre of the main lobe of the beam) receive the main weight. As a consequence, the theoretical and the measured patterns of received power coincide almost perfectly close to the peak of the pattern, while the differences in the low power parts of the pattern have practically no effect. The logarithmic minimization attempts to also minimize differences in the low power parts of the pattern, thus giving perhaps too much weight to the power values close to the noise level. Thus, if we aim to get good estimates for the HPBW, linear minimization should be used.

## 2.2 Horn measurements

### 2.2.1 Beam pattern

In order to verify the solar measurements, the real beam pattern of the radar antenna was measured during autumn 2003 with a standard gain horn antenna. The setup is sketched in Fig. 4. The horn antenna was placed on the top of a fire department tower located at a distance of 550 meters from the radar site at an elevation of 2.3°. A microwave signal generator capable of producing 15 dBm power was used as a transmitter.

The maximum power received with the radar antenna during this measurement was −52 dBm, which leaves approximately a 50 dB margin to observe side lobes before the noise obscures the signal.

At the radar site, an RVP7 linear IF receiver/signal processor was used with an equivalent number of 2048 samples

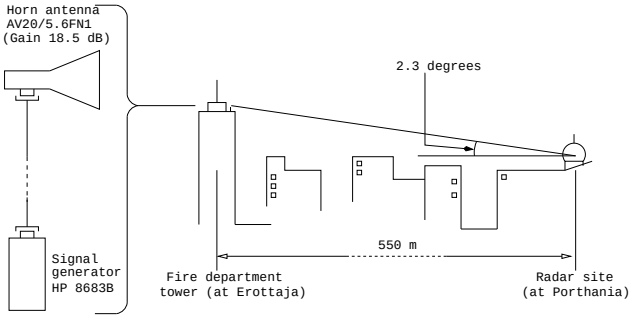


**Fig. 4.** The setup of the horn antenna measurement.

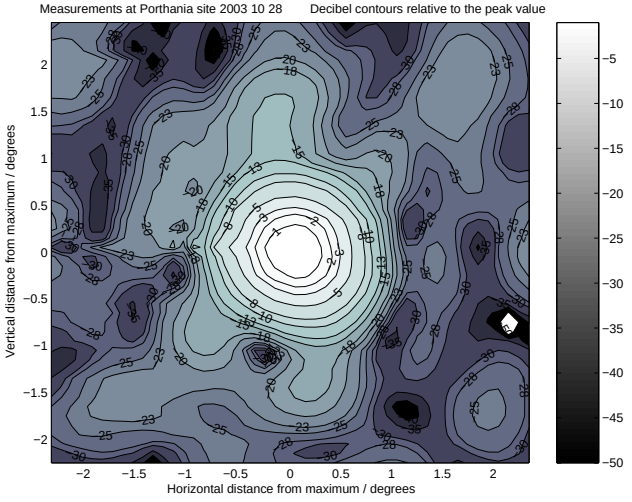


**Fig. 5.** Measured two-dimensional beam pattern of the radar antenna.

integrated for each measurement point. The radar antenna was rotated continuously 360° counter clockwise in azimuth while its elevation was increased by approximately 0.1° after every full revolution. The beam pattern is presented in Fig. 5, which shows that it is slightly elliptical with a tilted main axis.

In order to compare the 2-D horn measurements and solar measurements from single inclined tracks, the 2-D pattern was investigated by taking linearly interpolated intersections with various inclination angles between −90° and +90°. A Gaussian function was fitted to these curves to obtain the HPBWs (solid line in Fig. 7). Fitting was also done on a logarithmic scale to get the lowest estimate for the HPBWs (dash-dot line in Fig. 7). The highest estimate was found by solving the HPBW without any fitting, by measuring directly the angular distance between the half-power points (dashed line in Fig. 7). The peak around zero inclination is due to an error in the azimuth position data of the radar antenna. The same effect can also be seen in the form of irregularities on the left-hand side of the main lobe in Fig. 5.

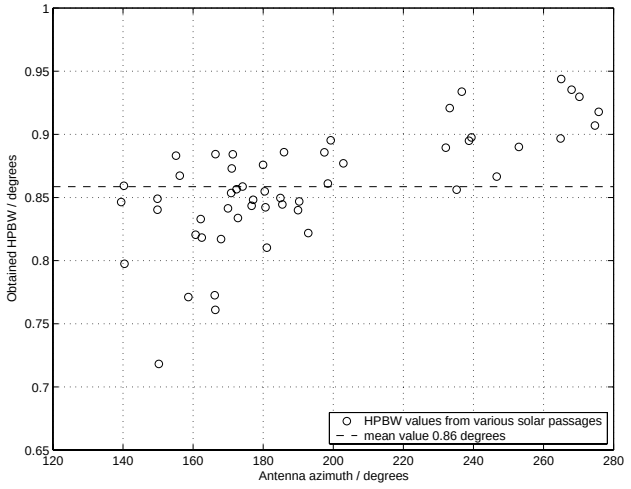


**Fig. 6.** HPBW obtained from solar measurements as a function of azimuth angle.

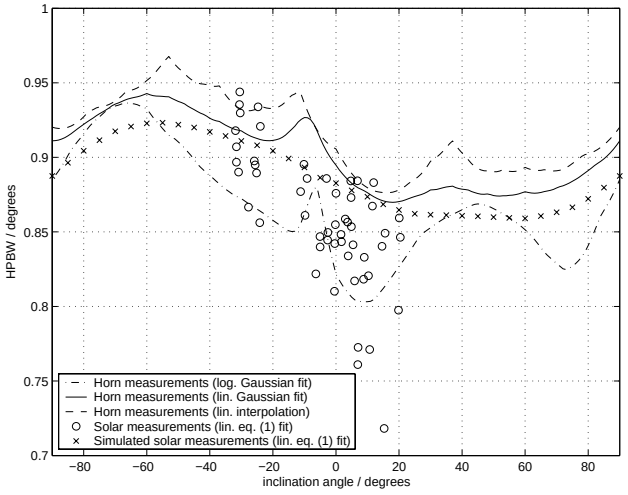


**Fig. 7.** HPBWs as a function of the inclination angle across the beam. Combined results of horn antenna measurements, solar passages (circles) and computer simulations (crosses).

#### 2.2.2 Antenna gain

Measurements to determine the antenna gain were performed during spring 2004, the setup being mostly as in Fig. 4. Measurements were done reciprocally, in other words by transmitting with the horn antenna and receiving with the radar antenna and vice versa.

The mean value for the gain obtained from these measurements was 43.5 dB. This is approximately 1 dB lower than the factory measurements, in which the radome was not included. The manufacturer of the radome estimated its attenuation to be less than 0.5 dB.

After the dismantling of the radar, the attenuation was investigated with a separate radome segment and a pair of horn antennas. The mean value of these measurements was approximately 1.1 dB. It can thus be concluded that the gain of the antenna without the radome, 44.6 dB, is essentially the same as it was at the manufacturer's facility 20 years ago.

## 3 Results

### 3.1 General

Equation (1) was fitted to single solar passages to obtain the HPBW for each measurement. The resulting beam widths are plotted in Fig. 6 as a function of antenna azimuth. At 180° the Sun is in the south at its highest elevation and intersects the beam nearly horizontally. On the left-hand side the Sun is rising and on the right-hand side it is setting. As the inclination angle of the solar trajectory is unambiguously related to the azimuth, this set of points offers direct indication of the ellipticity of the beam. In Fig. 7, the same data points are presented as a function of the inclination angle and are plotted for comparison in same figure with results from the horn antenna measurements. The decreasing trend as the inclination angle increases is clearly observable from the solar measurements, indicating the elliptical main lobe shape of the radar antenna.

The mean value for the HPBW with a linear fitting procedure was 0.86°, which is 0.04° less than the mean value from the real beam pattern (0.90°, solid line in Fig. 7). One reason for this is that the fitting procedure of the analytical method tends to produce a curve which slightly differs from the measured values around the maximum. In the numerical solution an attempt was made to force the fitted curve to coincide with the maximum of the measured values, yielding wider beam widths (mean value 0.88°).

As can be seen, the HPBW values for a single inclination angle vary within a relatively large interval (approximately ±0.03°). These variations are discussed in the following section.

### 3.2 Error sources

#### 3.2.1 Simulations

An ideal version of a solar passage was simulated using the real beam pattern of the antenna. The Sun was simulated as a circular disk of constant brightness. The solar trajectory was simulated with several inclination angles between −90° and +90°. Equation (1) was fitted to these simulations on a linear scale. The beam widths obtained are plotted in Fig. 7. Note that in this simulation, a real calibration curve of the receiver was not used and no pointing errors were included. Thus, this result represents an ideal noiseless situation with a purely linear receiver response and a perfect antenna pedestal.

As can be seen, the simulated result gives in general a slightly narrower beam width than the real data, but not as much so as the solar measurements. This indicates that although some limiting assumptions were made in Eq. (1), it still works relatively well, and most of the deviations in the results are caused by other nonidealities.

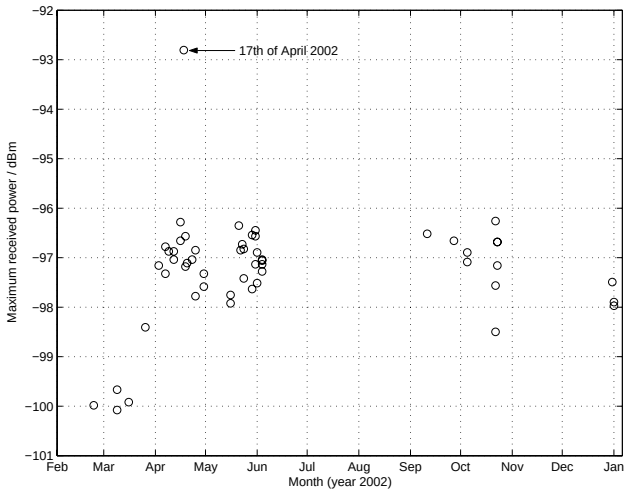


**Fig. 8.** Maximum received power as a function of measurement date.

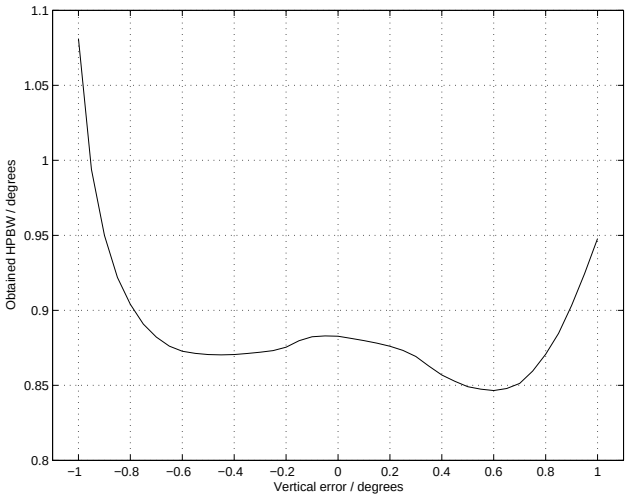


**Fig. 9.** Effect of vertical pointing error in HPBW.

### 3.2.2 Power variations

The power variations can be divided into two categories, namely, short and long time-scale variations. Variations on short time-scales appear within the time of a single solar passage (i.e less than 10 minutes), yielding data which do not behave as Eq. (1) predicts. This is because the term $I$ is essentially no longer constant. Such variations are usually linked with rapid solar events, but can also be caused by atmospheric effects like clouds and rain.

Long-term variations are illustrated in Fig. 8, where the maximum power of each passage is plotted as a function of date. With a few exceptions, the normal interval for the variation is approximately $\pm 1$ dBm. Provided that $I$ remains constant during a single measurement, the variation of $I$ between different passages does not affect the HPBW obtained via Eq. (1). However, a slight dependence between the value of HPBW obtained and maximum power was detected. This is most likely caused by non-ideality in the receiver response when the signal is close to the noise level.

Possible causes for long-term variations include solar activity and receiver stability. The atmospheric attenuation also varies, but this is systematic as a function of the antenna elevation.

### 3.2.3 Activity of the Sun

From the point of view of these solar measurements, three categories of solar activity are separated: long-term variations, solar radio bursts and spatial topology of the solar intensity on the solar disk.

The first factor varies typically on time scales from several days to several years, owing mainly to the 27-day rotation period, evolution of single active regions and the 11-year activity cycle of the Sun (Krueger, 1979). In these measurements the rotation and active regions are obviously dominant.

Solar radio bursts are connected with the sudden eruptions of active regions and are typically very impulsive, lasting from a few minutes to a few hours (Urpo et al., 2003a,b). The high power observation of 17 April 2002 in Fig. 8 is an example of such an event. The received power is 4 dBm higher than normal. At the same time, an independent measurement was done with a 11.7 GHz solar microwave radiometer located at Metshovi radio observatory in Finland. This indicated that the solar passage was measured during the falling edge of a radio burst and that the intensity decreased less than 1 dB during the passage. This did not significantly affect the HPBW obtained, i.e. 0.85°.

Not only during a radio burst but also in silent situations there are usually a few more intense regions on the solar surface having intensities of an order of 3 dB higher than the surroundings (Das et al., 1999). Another phenomenon is the dependence of the effective solar radius at radio frequencies on short time-scale radiation intensity. According to Das et al. (1999), this might be as much as 20 percent, yielding a $\pm 0.02°$ variation in HPBW, according to computer simulations.

### 3.2.4 Pointing errors

Vertical pointing errors were investigated by simulating measurements in which a horizontal solar trajectory passed the beam pattern with a certain vertical pointing error (see Fig. 1 for definition of vertical error). The result is plotted in Fig. 9. If the pointing error is less than $\pm 0.3°$, the effect on the variation of the HPBW is less than $\pm 0.015°$. The high values at the edges of this plot are caused by the interference of a complex pattern of first sidelobes.

## 4 Concluding remarks

According to the results obtained, the Sun can be used to determine the HPBW with an accuracy of $\pm 0.03°$. The elliptic

main lobe shape as well as the angle of the principal axis of the ellipse can be approximated from the results.

Random variations in the HPBW were explained by pointing errors, solar activity and other power variations. The errors caused by power variations are a consequence of the non-ideal receiver response and are thus largely eliminated when using a modern digital IF receiver. The effect of pointing errors can be reduced by using solar measurements first to determine azimuth and elevation errors of the antenna pedestal, but in order to do this properly, a precise scanning capability is needed. However, according to the simulations, the pointing errors did not cause severe errors in HPBW.

The effect of solar activity was also shown to be a minor problem. Even in the case of a strong solar radio burst, there was not a significant change in the HPBW obtained, as the passage was measured during the falling edge of the burst. The only possible problem is the rapid onset of a strong radio burst. However, a total of 53 solar passages were measured during this campaign and only one significant solar radio burst occurred simultaneously, meaning basically that such events are very unlikely. Furthermore, they can be detected from the data by monitoring the level of the received power.

*Acknowledgements.* The authors would like to acknowledge Metshovi Radio Observatory and Prof. Emer. Seppo Urpo for the solar radio data used in this project and the Vilho, Yrjö and Kalle Väisälä Foundation for a scholarship making this research possible. Financial support was also received from TEKES.

## References

Arnott, N. R., Richardson, Y. P., Wurman, J. M., and Lutz, J.: A Solar Alignment Technique for Determining Mobile Radar Pointing Angles, 31st Conference on Radar Meteorology, AMS, 491–493, 2003.

Das, T. K., Sarkar, H., Sen, A. K., The Ratio of the Radio and Optical Diameters of the Sun at Centimeter Wavelengths, Solar Physics, Kluwer Academic Publishers, 194: 155–163, Netherlands, 2000.

Frush, C. L.: Using the Sun as a Calibration Aid in Multiple Parameter Meteorological Radars, 22nd Conference On Radar Meteorology, AMS, 306–311, 1984.

Hubbert, J. C., Bringi, V. N., and Brunkow, D.: Studies of the Polarimetric Covariance Matrix. Part I: Calibration Methodology, J. Atmos. Oceanic Technol., 20, 696–706, 2003.

Krueger, A.: Introduction to Solar Radio Astronomy, D. Reidel Publishing Company, Dordrecht, Holland, 330 p., 1979.

Kuz'min, A. D. and Salomonovich, A. E.: Radioastronomical Methods of Antenna Measurements, Academic Press, New York, 182 p., 1966.

Leskinen, M., Puhakka, P., and Puhakka, T.: A method for estimating antenna beam parameters using the Sun, Proceedings of ERAD (2002), Copernicus, 318–323, 2002.

Puhakka, P.: Total Power Radiometer in Solar Microwave Research, Master's Thesis in Physics (written in Finnish), University of Helsinki and Metsähovi Radio Observatory, 70 p., 2002.

Smith P. L.: Calibration of weather radars, 30th Radar Meteorology Conference Proceedings, A. M. S., 60–65, 1968.

SOLPOS: www.nrel.gov/midc/solpos, Measurement and Instrumentation Data Center (MIDC), National Renewable Energy Laboratory, United States, 2004.

Urpo, S., Puhakka, P., Oinaskallio, E., Mujunen, A., Peltonen, J., Rönnberg, H., Hurtta, S., Tornikoski, M., Teräsranta, H., and Könönen, P.: Selected Radio Maps and Major Solar Flares Measured at Metsähovi in 1996–2001, Metsähovi Publications on Radio Science, HUT-MET-46, Metsähovi Radio Observatory, Helsinki University of Technology, Espoo, 78 p., 2003.

Urpo, S., Puhakka, P., Oinaskallio, E., Mujunen, A., Peltonen, J., Rönnberg, H., Hurtta, S., Tornikoski, M., Teräsranta, H., and Könönen P.: Selected Radio Maps and Major Solar Flares Measured at Metsähovi in 2002, Metsähovi Publications on Radio Science, HUT-MET-47, Metsähovi Radio Observatory, Helsinki University of Technology, Espoo, 89 p., 2003.

Whiton, R. C., Smith, P. L., and Habuck, A. C.: Calibration of weather radar systems using the Sun as a radio source, 17th Conference on Radar Meteorology, A. M. S., 60–65, 1976.

Wilson, J. W.: Observations of radome transmission losses at 5 cm wavelengths, Preprints 18th Conference on Radar Meteorology, A. M. S., 288–291, 1978.